Phosphorylated GSK-3β protects stress-induced apoptosis of myoblasts via the PI3K/Akt signaling pathway

MEIXI LIU[1,2], XIA HUANG[3], YIHONG TIAN[1,2], XIAO YAN[1], FANG WANG[4], JUNBO CHEN[2], QI ZHANG[2], QIANG ZHANG[1] and XIAO YUAN[1]

[1]Department of Orthodontics II, The Affiliated Hospital of Qingdao University; [2]School of Stomatology of Qingdao University; [3]Department of Nursing and Hospital Infection Management, The Affiliated Hospital of Qingdao University, Qingdao, Shandong 266000; [4]Department of Orthodontics, Xiaoshan Branch of Hangzhou Stomatology Hospital, Hangzhou, Zhejiang 310000, P.R. China

Received May 27, 2019; Accepted February 17, 2020

DOI: 10.3892/mmr.2020.11105

Abstract. Facial jaw muscle is involved in the occurrence, development, treatment and maintenance of maxillofacial deformities. The structure and function of this tissue can be altered by changes in external stimuli, and orthodontists can regulate its reconstruction using orthopedic forces. The PI3K/Akt signaling pathway is most well-known for its biological functions in cell proliferation, survival and apoptosis. In the present study, the effects of the PI3K/Akt signaling pathway in cyclic stretch-induced myoblast apoptosis were investigated. For this purpose, L6 rat myoblasts were cultured under mechanical stimulation and treated with the PI3K kinase inhibitor, LY294002, to elucidate the role of the PI3K/Akt signaling pathway. Cells were stained with Hoechst 33258 to visualize morphological changes and apoptosis of myoblasts, and western blotting was performed to detect expression of Akt, phosphorylated (p)-Akt (Ser473), glycogen synthase kinase 3β (GSK-3β) and p-GSK-3β (Ser9). After addition of PI3K inhibitor, the expression of total Akt and GSK-3β did not significantly differ among groups; however, the levels of p-Akt and p-GSK-3β were lower in inhibitor-treated groups than in those treated with loading stress alone. In addition, the rate of apoptosis in myoblasts subjected to cyclic stretch increased in a time-dependent manner, peaking at 24 h. Collectively, it was also demonstrated that the PI3K/Akt/GSK-3β pathway plays an important role in stretch-induced myoblast apoptosis.

Introduction

A wide variety of functional appliances, such as the activator, twin-block and Herbst types, are used to correct Class II skeletal and occlusal disharmonies in patients undergoing growth and development (1). Functional appliances are particularly popular for correcting Class II malocclusion in growing children, as well as for improving undesirable facial profiles (2,3). Clinically, functional and fixed appliances are used to treat Class II division 1 malocclusions characterized by lower jaw inadequacy, allowing the mandible to extend forward in a fixed position to stimulate mandibular growth (4). Several studies have reported that functional appliances promote movement of the teeth and help to achieve proper facial muscle function (5,6). With the use of functional appliances, the patient's neuromuscular and skeletal systems undergo adaptive modifications. However, despite the widespread use of such functional appliances, the precise mechanism of action responsible for these modifications, as well as the skeletal and dental effects, remain unclear. The mechanisms underlying tensile muscle structural adaptability in response to functional instruments have received a great deal of interest. Research has suggested that skeletal muscle proliferation, differentiation, migration and apoptosis occur as a result of significant levels of mechanical stretch (7). Mechanical stretching of skeletal muscle initiates a series of cellular responses that can cause stem or progenitor cells to enter the cell cycle, divide, differentiate and fuse with other cells to repair damaged areas (8,9), or alternatively to undergo apoptosis (10,11). Previous studies have focused on the response of cell proliferation and differentiation to adaptive mechanical stretching of muscle cells (12,13). However, as accumulating evidence has revealed that apoptosis plays a major role in the adaptation of skeletal muscle function, more attention has been given to stretch-induced apoptosis (14). Therefore, elucidating the mechanism by which myoblast apoptosis is induced by mechanical stress is essential for improving the understanding of the adaptive mechanisms of skeletal muscle function. This in turn could help to maximize stress-induced skeletal muscle remodeling.

Apoptosis is a distinctive and physiologically important mode of programmed cell death, and plays a crucial role in homeostasis, normal development and elimination of potentially pathological cells from the body (15,16). One important

Correspondence to: Professor Xiao Yuan or Mr. Qiang Zhang, Department of Orthodontics II, The Affiliated Hospital of Qingdao University, 16 Jiangsu Road, Qingdao, Shandong 266000, P.R. China
E-mail: yuanxiaoqd@163.com
E-mail: zqzbyzh@163.com

Key words: PI3K, Akt, cyclic stretch, apoptosis, myoblast

trigger of the apoptotic response is overload mechanical stretch (17). The duration and intensity of mechanical stretching determine whether a cell will survive the stress by adapting, or instead undergo autophagy or apoptosis due to unacceptably high levels of stress. There are three main apoptotic pathways: The death receptor depentent pathway (extrinsic pathway), the mitochondrial-mediated pathway (intrinsic pathway) and the endoplasmic reticulum-mediated pathway (14). Previous evidence has implicated the PI3K/Akt pathway in apoptosis (18). However, the involvement of PI3K/Akt signaling in mechanically induced muscle apoptosis has not been clearly demonstrated.

The PI3K/Akt pathway is a critical signaling pathway that mediates a variety of cellular functions, such as survival, proliferation, migration and differentiation (19). PI3K can be activated by a wide range of environmental stimuli (20). After activation of PI3K, phosphoinositide-dependent protein kinase-1 recruits Akt to the cell membrane and activates it (21). The activation of Akt controls a variety of biological responses, such as the stimulation of cell proliferation and inhibition of apoptosis (22,23). The mitochondria play an important role in the regulation of apoptosis and necrotic death, and the opening of the mitochondrial permeability transition pore (MPTP) is considered to be a critical regulator of cell death. However, the specific mechanism underlying this remains unclear (24). The PI3K/Akt pathway is involved in MPTP opening during cardiomyocyte apoptosis induced by oxidative stress (23). To date, however, research addressing the role of the PI3K/Akt pathway in stretch-induced apoptosis of myoblasts has been limited.

In the present study, rat L6 cells were used to explore stretch-induced apoptosis in skeletal muscles and investigate the involvement of the PI3K/Akt pathway. Furthermore, a specific inhibitor of PI3K/Akt was used to investigate the role of the PI3K/Akt pathway in this process. L6 cell structure, ultrastructure and levels of apoptosis were measured by microscopy, and protein expression levels were determined by western blotting (WB).

Materials and methods

Cell culture. L6 rat myoblasts (The Cell Bank of Type Culture Collection of the Chinese Academy of Sciences) were cultured in a humidified incubator at 37˚C in an atmosphere containing 5% CO_2. Cultures were grown in DMEM (HyClone; GE Healthcare Life Sciences), containing 10% fetal bovine serum (HyClone; GE Healthcare Life Sciences), 100 U/ml penicillin and 100 μg/ml streptomycin. Growth medium was replaced every other day. When the cells reached 80% confluence, they were digested with 0.25% trypsin and passaged at a split ratio of 1:2. Cells were then seeded in growth medium into each well of a 6-well plate (BioFlex; Flexcell International Corporation) at $3x10^5$ cells/well.

Stretch loading. L6 cells were suspended in growth medium, seeded at a density of $3x10^5$ cells/well in flexible bottom 6-well plates and assigned to one of the following groups: Control, 2, 6, 12 and 24 h. Except for stretching, the control group was treated in the same way as the mechanically stretched group. Cells in the 2, 6, 12 and 24 h groups were subjected to a cyclic strain of 15% elongation at a frequency of 10 cycles/min for the indicated periods of time on a computer-controlled vacuum stretch apparatus (FX-4000T™ Tension Plus System; Flexcell International Corporation). Each cycle consisted of a 3-sec stretching period followed by a 3-sec relaxation period. Experiments were repeated three times. Cell growth was examined and imaged with an inverted microscope using at a magnification of x10x (Eppendorf).

Hoechst staining assay. Cells were stained using the Hoechst Staining Kit (Beyotime Institute of Biotechnology), Briefly, L6 rat skeletal muscle myoblasts were fixed for 10 min at room temperature or overnight at 4˚C with 0.5 ml/well fixation buffer, and then washed twice in PBS. After addition of Hoechst 33258 (5 ml/well), the cells were placed at 37˚C in the dark to stain for 5 min and then washed twice again with PBS. Apoptotic cells were visualized by a fluorescence microscope (Eppendorf). The apoptotic index was calculated as the percentage of apoptotic nuclei per total nuclei number per field.

Assessment of MPTP opening. MPTP opening was assessed by using the calcein-AM/cobalt method. The cells were seeded in 6-well plates; after cyclic stretching, the cells were washed twice with PBS and stained with 5 μl calcein-AM working solution (Cell Stain Buffer 1:500 diluted 1mM Calcein AM stock solution) for 30 min at 37˚C. After two washes with PBS, the cells were analyzed by flow cytometry (Epics XL; Beckman-Coulter). The flow cytometer showed the proportion of apoptotic area (V1-L) and Calcein fluorescence area (V1-R) of myoblast in each group.

WB analysis. After cyclic stretching, the cells were harvested in RIPA lysis buffer [50 mM Tris (pH 7.4), 1 mM EDTA, 1% TritonX-100, 150 mM NaCl, 1 mM phenylmethanesulfonyl fluoride and 1X protease inhibitor]. Lysates were centrifuged at 12,000 x g for 10 min at 4˚C, and protein concentrations were determined using the bicinchoninic acid method. Protein extracts (30 μl/well) were separated on a 10% gel via SDS-PAGE and transferred to PVDF membranes. Membranes were blocked with 10% instant non-fat dry milk for 1 h at room temperature and then incubated with primary antibody purchased from Cell Signaling Technology, Inc.: Akt (1:1,000; rabbit; cat. no. 9331), phosphorylated (p)-Akt (1:1,000; rabbit; cat. no. 9271), GSK-3β (1:1,000; rabbit; cat. no. 9315), p-GSK-3β (1:1,000; rabbit; cat. no. 9336) and GAPDH (1:1,000; rabbit; cat. no. 5174) overnight at 4˚C. The membranes were washed three times for 5 min each with 10% TBS- 0.1% Tween 20 and then incubated with the goat anti-rabbit IgG-HRP secondary antibody conjugated with horseradish peroxidase (1:2,000; rabbit; cat. no. CW0103S, ComWin Biotech Co.) for 45-60 min at room temperature. Protein bands on the membranes were visualized on an enhanced chemiluminescence machine (Bio-Rad Laboratories, Inc.). and analyzed using Quantity One software version 4.6.6.(Bio-Rad Lbaoratories, Inc.)

Inhibition of PI3K/Akt signaling using LY294002. To determine whether PI3K/Akt signaling was involved in stretch-induced apoptosis, cells were treated with the

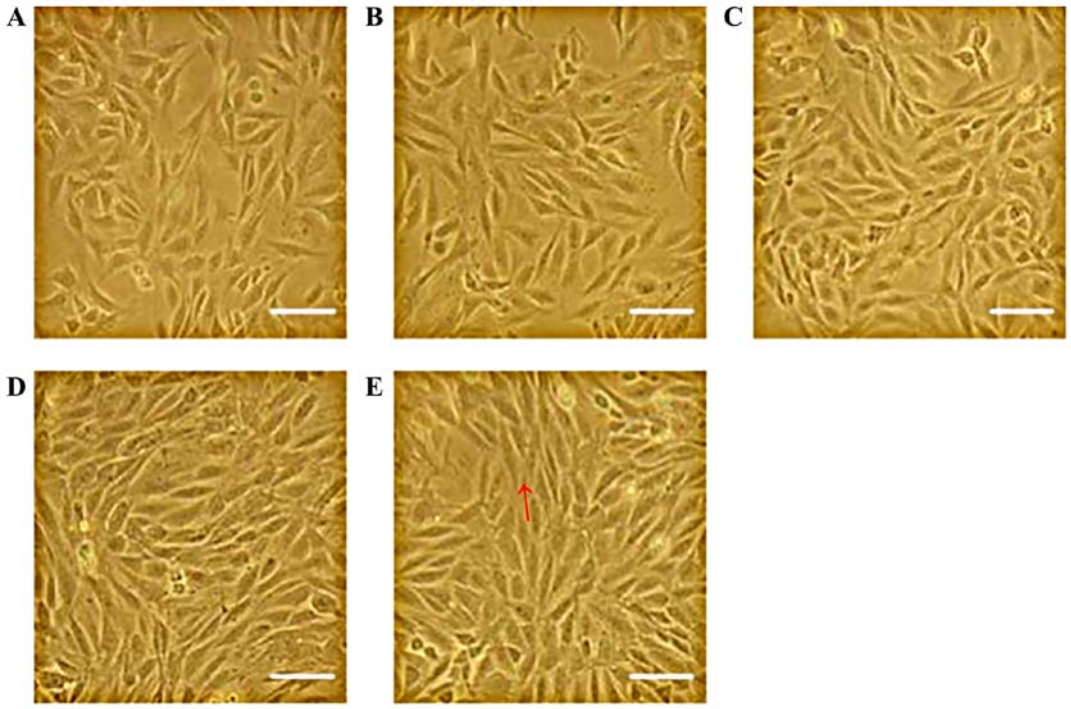

Figure 1. Changes in rat L6 myoblast morphology during mechanical stretching. (A) Unstretched group: cells are disorganized. Cells stretched for (B) 2, (C) 6, (D) 12 or (E) 24 h, respectively. After cyclic stretch was applied, myoblasts tended to align in the direction of the force field. Scale bar, 200 μm.

PI3K/Akt signaling inhibitor, LY294002 (ApexBio). Cells were treated with 20 μM LY294002 (2 μl/well) for 2 h prior to cyclic stretching. Apoptosis was assessed by Hoechst staining and opening of the MPTP, and levels of Akt, phosphorylated (p)-Akt, GSK-3β and p-GSK-3β were assessed by WB.

Statistical analysis. All experiments were performed ≥3 independent experiments performed in duplicate, and data are expressed as mean ± SD. Statistical significance of multiple groups was determined by two-way analysis of variance with post hoc Bonferroni test (SPSS version 17.0). Differences were considered statistically significant when $P<0.05$.

Results

Effect of mechanical stretch on the shape of L6 myoblasts. Images captured using an inverted microscope showed that the unstretched, plate-attached cells mainly possessed a spindle and irregular triangle-like morphology. However, after mechanical stretch for ≥2 h, the cells were more tightly aligned in the direction of the force field (Fig. 1). The longer the stretch interval, the more clear this phenomenon was, suggesting that the cells were stretched effectively.

Effect of high levels of mechanical stretch on apoptosis. Hoechst 33258 is a convenient and popular nuclear counterstain that emits blue fluorescence when it binds to DNA. Accordingly, it is used for general counterstaining, as well as for studies of apoptosis and the cell cycle. In this study, Hoechst staining was used to observe the effects of different stretch times on apoptosis. In the present study, cells were cyclically stretched for 2, 6, 12 or 24 h. Stretch loading consisted of 15% elongation at a frequency of 10 cycles/min. As shown in Fig. 2, the number of apoptotic cells in the mechanical stretch-treated group increased in quantity relative to the control group. Stained apoptotic cells exhibited dense, bright fluorescent chromatin in their nucleus, whereas the nuclei of normal cells appeared oval or round, and emitted a uniformly dispersed blue fluorescence. Nuclear condensation, fragmentation and apoptotic bodies gradually increased in frequency starting after 2 h, peaking after 24 h, indicating that the cells were undergoing apoptosis. The apoptotic index, defined as the percentage of nuclei in each region that were apoptotic, increased with time; after continuous stretch for 24 h, apoptotic bodies could be observed in the stretch-treated group but were less abundant in the control group.

In apoptosis, Bax has been widely recognized as the most representative proapoptotic protein of Bcl-2 family proteins (25). Caspase-3 has also widely accepted as a marker of most types of apoptosis (26). In the present study, protein expression of Bax and Caspase-3 was detected via WB. As shown in Fig. 3, an increase in Bax and Caspase-3 protein expression was observed after 2 and 12 h of mechanical loading, respectively, which increased gradually in a time-dependent manner. The ratio of Bax and Caspase-3 to GAPDH are displayed in Fig. 3B. Taken together, these results suggested that the mechanical loading condition promotes myoblast apoptosis in a time-dependent manner.

To further investigate the effects of mechanical stretch on the regulation of apoptosis, the opening of the MPTP, a useful method for monitoring the apoptotic rate in most cell types, was tested. MPTP function can be measured by monitoring its fluorescence intensity via flow cytometry. The

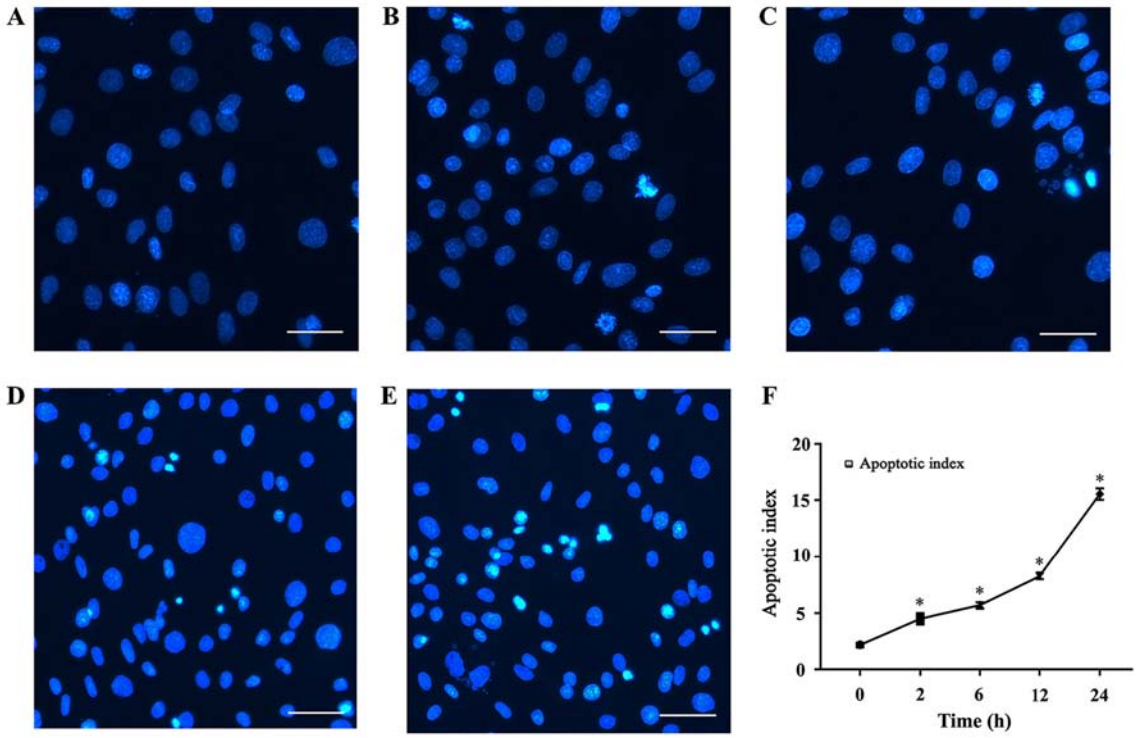

Figure 2. Apoptosis of rat L6 myoblasts stained with Hoechst 33258 after cyclic mechanical stretch. (A) Unstretched control cells; cells stretched for (B) 2, (C) 6, (D) 12 or (E) 24 h, respectively. Scale bar, 100 μm. The nuclei of apoptotic cells were bright blue and strongly fluorescent, whereas the chromatin of unstretched cells was light blue with uniform fluorescent dispersion, and the nuclei were round or oval. Apoptotic bodies were observed after continuous stretching for 24 h, and the proportion of apoptotic cells increased in a time-dependent manner. (F) Apoptotic index, calculated as the percentage of nuclei in each region that were apoptotic. Values represent mean ± SD of at least three independent experiments. *P<0.05 vs. unstretched control cells.

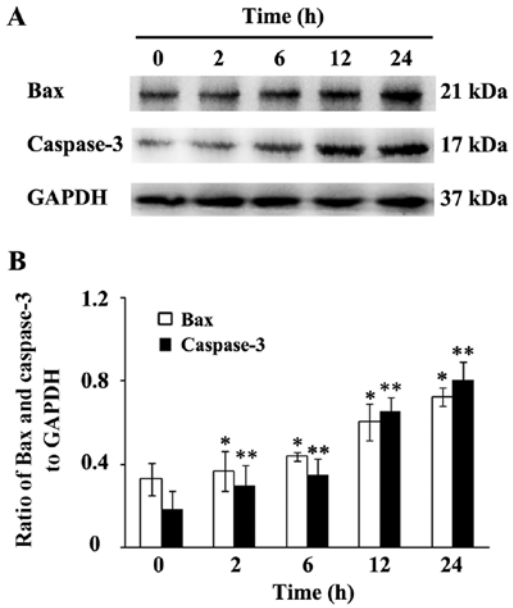

Figure 3. Western blot analysis of Bax and Caspase-3 protein expression at different stretching times. (A) Western blotting was performed for Bax and Caspase-3, with GAPDH as a loading control. (B) Ratios of Bax and Caspase-3 to GAPDH. The protein expression level of Bax and Caspase-3 increased with longer stretching times, and reached the highest after 24 h stretch. Values represent mean ± SD of at least three independent experiments. *P<0.05, **P<0.01 vs. unstretched control cells.

number of cells in the proportion of apoptotic area (V1-L) was the lowest in the control group. As the mechanical stretch time increased, the number of cells in V1-L also increased, reaching a maximum after 24 h (Fig. 4). The proportion of cells in V1-L represents the proportion of apoptotic cells; these findings demonstrated that cyclic stretch can induce myoblast apoptosis in a time-dependent manner.

Activation of the PI3K/Akt signaling pathway by mechanical stretch. Activation of PI3K is typically essential for cell proliferation and plays a central role in cellular signaling, leading to cell proliferation, survival, motility and secretion, as well as specialized cell responses, such as the respiratory burst of granulocytes (27). To determine whether mechanical stretch affects the PI3K/Akt signaling pathway in myoblasts, the protein expression levels of p-Akt and Akt by were measured by WB. In certain samples, LY294002, an inhibitor of the PI3K/Akt signaling pathway was added, and apoptosis was monitored by staining with Hoechst 33258 and detecting changes in the MPTP by flow cytometry. The aforementioned proteins were also detected via WB.

Inhibition of PI3K/Akt signaling on GSK3β dephosphorylation, mPTP opening and myoblast apoptosis. The apoptotic indices of each group of myoblasts are presented in Fig. 5. After stretching for 24 h and adding LY294002, myoblasts exhibited an elevated apoptotic index. However, myoblasts that were not exposed to stretch, or that were treated with LY294002 alone, had a lower apoptotic index

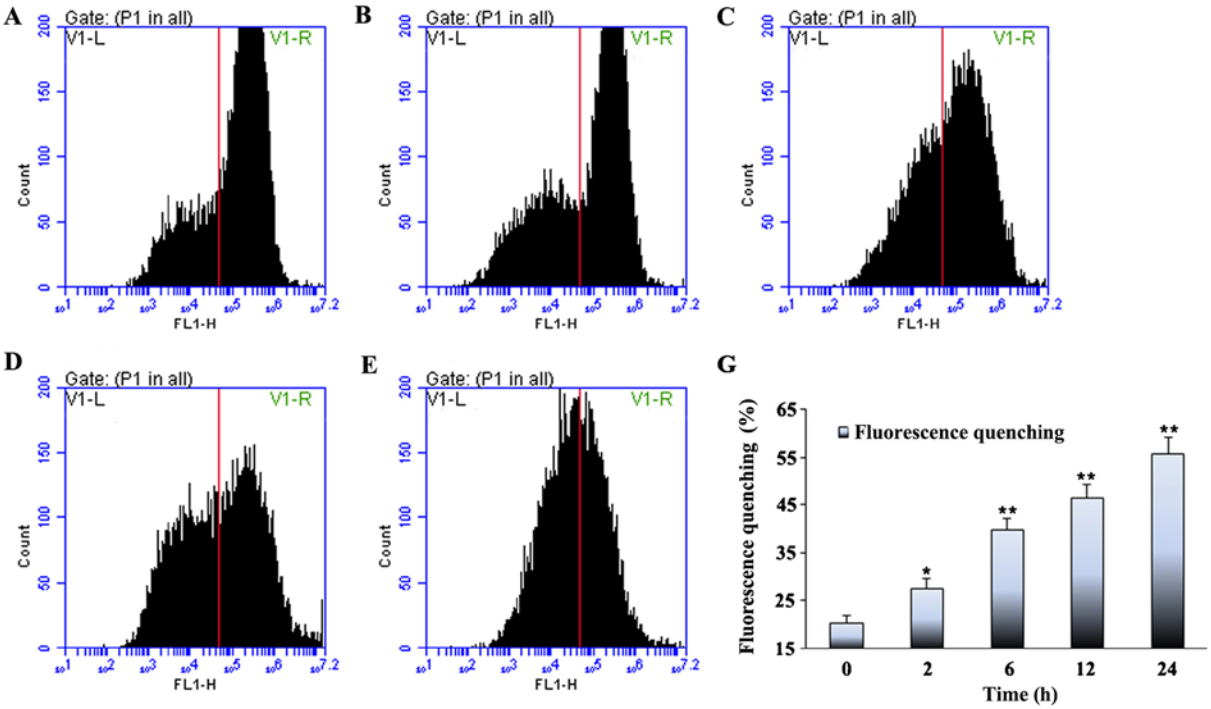

F **Proportion of apoptotic area (V1-L) and Calcein fluorescence area (V1-R)**

	0 h	2 h	6 h	12 h	24 h
V1-L	20.45±1.56	27.73±2.13	39.96±2.35	46.46±2.83	55.83±3.41
V1-R	79.55±2.78	72.27±3.04	60.04±3.36	53.54±3.28	44.17±2.63

Figure 4. Analysis of apoptosis by monitoring the opening of the mitochondrial permeability transition pore. Representative set of plots from flow cytometry of (A) unstretched control cells and cells stretched for (B) 2, (C) 6, (D) 12 or (E) 24 h, respectively. (F) Proportion of apoptotic area (V1-L) and Calcein fluorescence area (V1-R) of myoblast in each group. (G) Percentage fluorescence quenching, calculated as the area ratio of the apoptotic area. The percentage of fluorescence quenching increased with time. Values are presented as mean ± SD. *P<0.05, **P<0.01 vs. unstretched control cells. V1-L, calcein fluorescence-negative or apoptotic region; V1-R, fluorescence-positive region.

than stretch-treated myoblasts. The lowest apoptotic index was observed in non-stretched cells without LY294002 treatment.

GSK-3β is an important cell regulator of metabolism and an important regulator of cell proliferation, migration, cell death and immune function (28,29). Moreover, it is a major downstream target of PI3K/Akt signaling (30). To further assess the functional role of PI3K/Akt in stretch-induced apoptosis, a specific PI3K inhibitor LY294002 was used. The V1-L proportion was lower in the unstretched cells + LY294002 treatment compared with the unstretched cells without treatment, and higher in the 24 h stretched cells + LY294002 treatment compared with the 24 h stretched cells without treatment. The V1-L proportion was highest in the 24 h stretched cells + LY294002 treatment group (Fig. 6). The levels of total Akt and GSK-3β did not change when the stretch time was extended, whereas the levels of p-Akt and p-GSK-3β tended to decrease with stretch time; the p-proteins were least abundant at 24 h (Fig. 7). After the addition of the PI3K inhibitor, there was no difference between groups in the levels of total Akt and GSK-3β, whereas the levels of p-Akt and p-GSK-3β were lower in the inhibitor group than in the pure stretch group, and the levels of p-proteins in the inhibitor group were lowest after 24 h treatment with the inhibitor (Fig. 8). It was speculated that LY294002 inhibited the phosphorylation of GSK-3β in myoblasts under cyclic stress conditions, which led to the opening of MPTP and eventually cell apoptosis. Therefore, the results suggested that inhibition of the PI3K/Akt pathway plays a critical role in the dephosphorylation of GSK-3β, MPTP opening and mitochondrial apoptosis of myoblast cells under cyclic stress.

Discussion

In the present study, the involvement of the PI3K/Akt signaling pathway in apoptosis induced by cyclic stretch in rat L6 myoblasts was investigated. First, it was demonstrated that cyclic stretch consisting of 15% elongation at 10 cycles/min affected the morphology and induced apoptosis of rat L6 myoblasts. Second, it was shown that cyclic mechanical stretch can increase the opening of the MPTP, thereby increasing mitochondrial permeability. Furthermore, it was found that LY294002, a PI3K/Akt

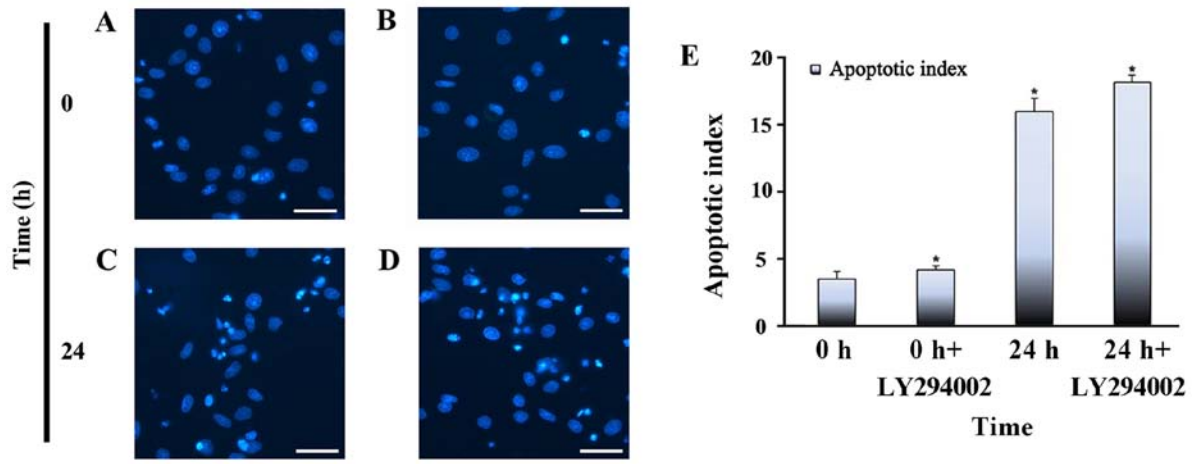

Figure 5. Rat L6 myoblast apoptosis observed by Hoechst 33258 staining. Cells were stretched for 24 h or unstretched (0 h), with or without the PI3K inhibitor LY294002. All cells were harvested at the end of 24 h. Scale bar, 100 μm. (A) Unstretched control; (B) unstretched control + LY294002; (C) 24 h stretch, without LY294002; and (D) 24 h stretch + LY294002. Nuclei of apoptotic cells were bright blue and strongly fluorescent, whereas the chromatin of normal cells was light blue with uniform fluorescence, and the nuclei were round or oval. (E) Apoptotic index, calculated as the percentage of nuclei in each region that were apoptotic. The number of apoptotic cells increased and apoptosis was more apparent in myoblasts treated with inhibitor compared with myoblasts not treated with inhibitor. Data are presented as the mean ± SD of ≥3 independent experiments. *P<0.05 vs. unstretched control cells.

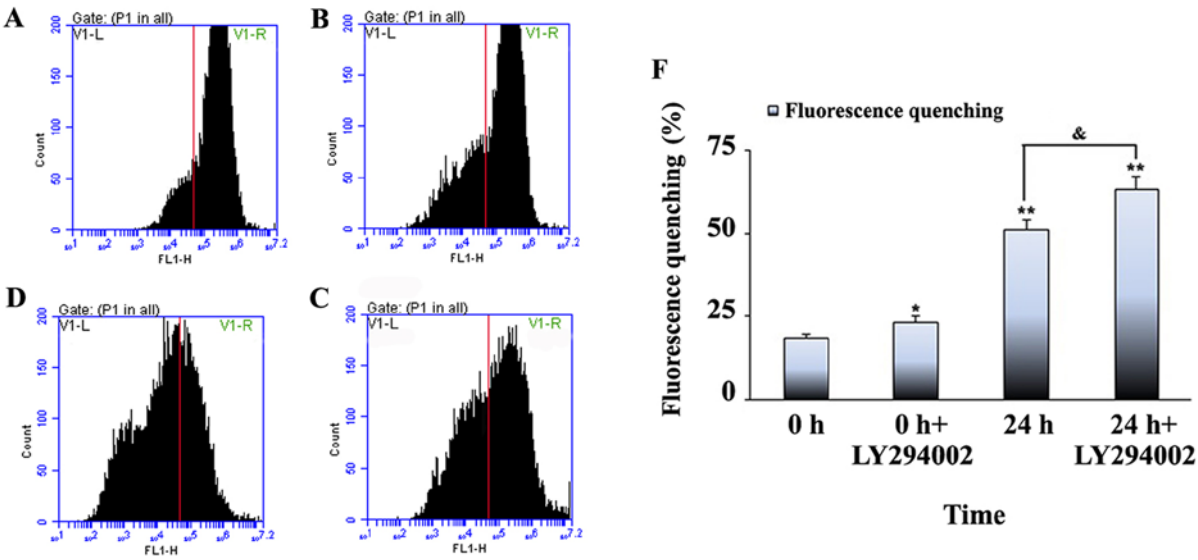

E **Proportion of apoptotic area (V1-L) and Calcein fluorescence area (V1-R)**

	0 h	0 h+LY294002	24 h	24 h+LY294002
V1-L	18.72±1.16	23.31±2.09	50.96±3.27	63.17±4.08
V1-R	81.28±3.25	76.69±3.21	49.04±2.71	36.83±2.04

Figure 6. Analysis of apoptosis by monitoring the opening of the mitochondrial permeability transition pore. Cells were stretched for 24 h or unstretched, with or without the PI3K inhibitor LY294002. All samples were harvested after 24 h. (A) Unstretched control; (B) unstretched control + LY294002; (C) 24 h stretch, without LY294002; and (D) 24 h stretch + LY294002. (E) Proportion of apoptotic area (V1-L) and Calcein fluorescence area (V1-R) of myoblast in each group. (F) Percentage fluorescence quenching of myoblasts was higher with inhibitor than without inhibitor, and was highest in cells subjected to stretch with LY294002 for 24 h. Results represent mean ± SD of three experiments. *P<0.05, **P<0.01 vs. control. $^{\&}$P<0.05 vs. 24 h. V1-L, calcein fluorescence-negative or apoptotic region; V1-R, fluorescence-positive region.

signaling pathway inhibitor, partly promoted apoptosis caused by cyclic stretch in rat L6 cells.

Overloading mechanical stretch may cause injury or apoptosis in skeletal muscle (11). Several studies have shown

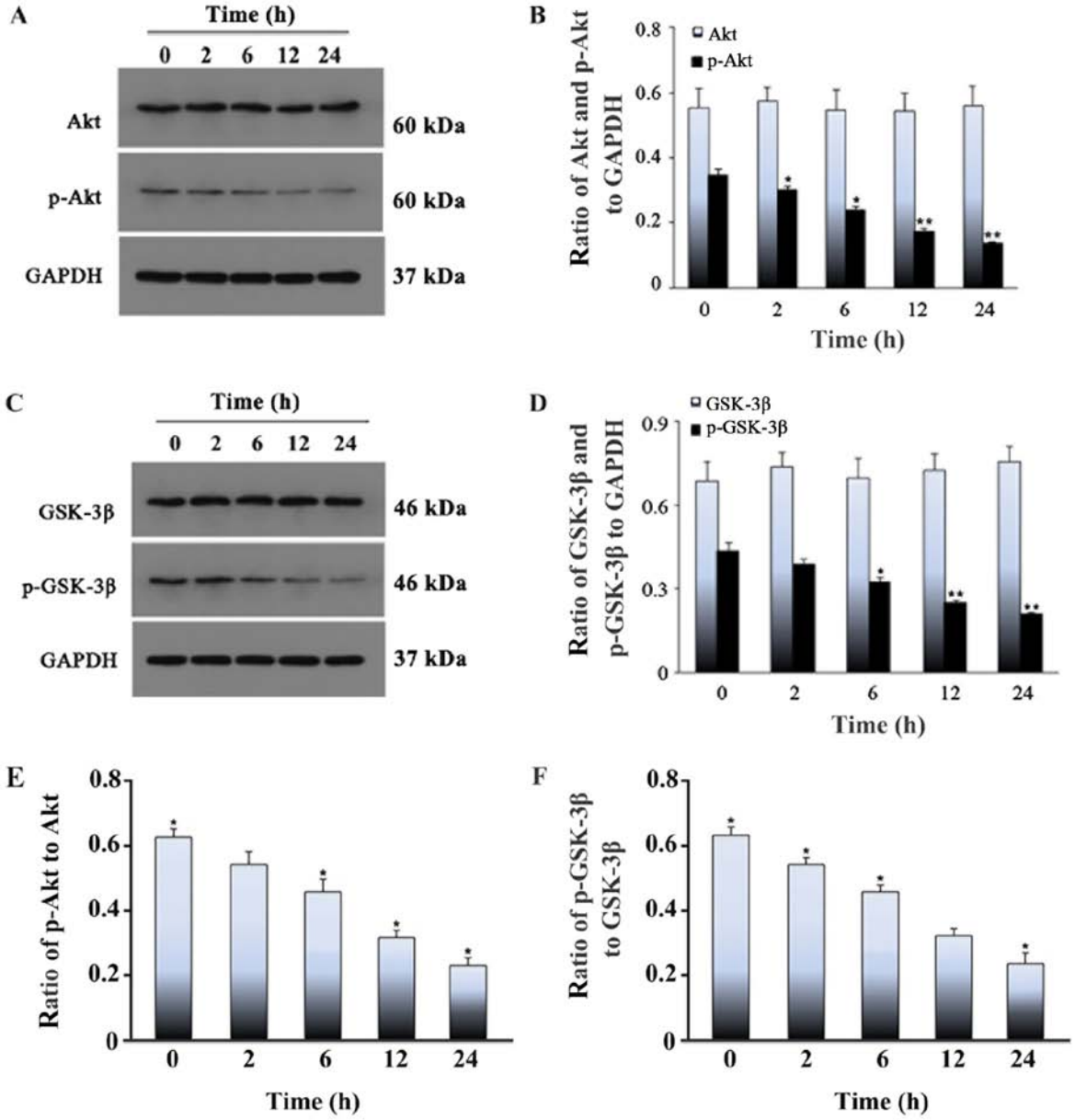

Figure 7. Effect of cyclic stretch on the levels of Akt, p-Akt, GSK-3β and p-GSK-3β in rat L6 myoblasts. Myoblasts were exposed to cyclic stretch for 0, 2, 6, 12 or 24 h, followed by western blotting. (A) Western blotting results of the protein expression of (B) p-Akt was significantly decreased over time, reaching a minimum level at 24 h, whereas the level of total Akt remained stable. (C) Western blotting results of the protein expression of (D) p-GSK-3β was significantly decreased over time, reaching a minimum level at 24 h, whereas the level of total GSK-3β protein remained stable. The ratio of (E) p-Akt to Akt and the ratio of (F) p-GSK-3β to GSK-3β. Values represent mean ± SD of three experiments. *P<0.05 vs. control; **P<0.01 vs. control. GSK-3β, glycogen synthase kinase 3β; p, phosphorylated.

that excessive stretch can seriously damage the structure and physiological function of cells (9). Our previous study reported that apoptosis increased with stretch time (31). In the present study, to test the hypothesis that excessive stretch would increase myoblast apoptosis, histopathological and staining changes were observed in cells subjected to cyclic stretch. Fluorescence microscopy revealed that myoblasts tended to align in the direction of the force field, and that this change became more pronounced as the stretch time increased. Hoechst 33258 staining results displayed changes in cell morphology. The structure of stretched L6 cells was markedly different from those of the control group, and contained condensed chromatin and apoptotic bodies. WB was also used to detect the expression level of Bax and Caspase-3: The results showed that cyclic mechanical stretch induces myoblast apoptosis in a time-dependent manner.

Next, it was shown that the PI3K/Akt signaling pathway was involved in mechanical stretch-induced myoblast apoptosis, and that treatment with LY294002 inhibited the PI3K/Akt signaling pathway. The PI3K/Akt signaling pathway plays a vital role in diverse cellular functions, such as the suppression of apoptosis and promotion of proliferation (32,33), as well as cell cycle progression (34). Phosphorylation of Akt is an important step in the process of apoptosis (35). Sussman (36) reported that phosphorylation of Akt facilitates cell survival and proliferation, and regulates multiple signaling pathways. On the other hand, GSK3β, an Akt substrate that plays critical

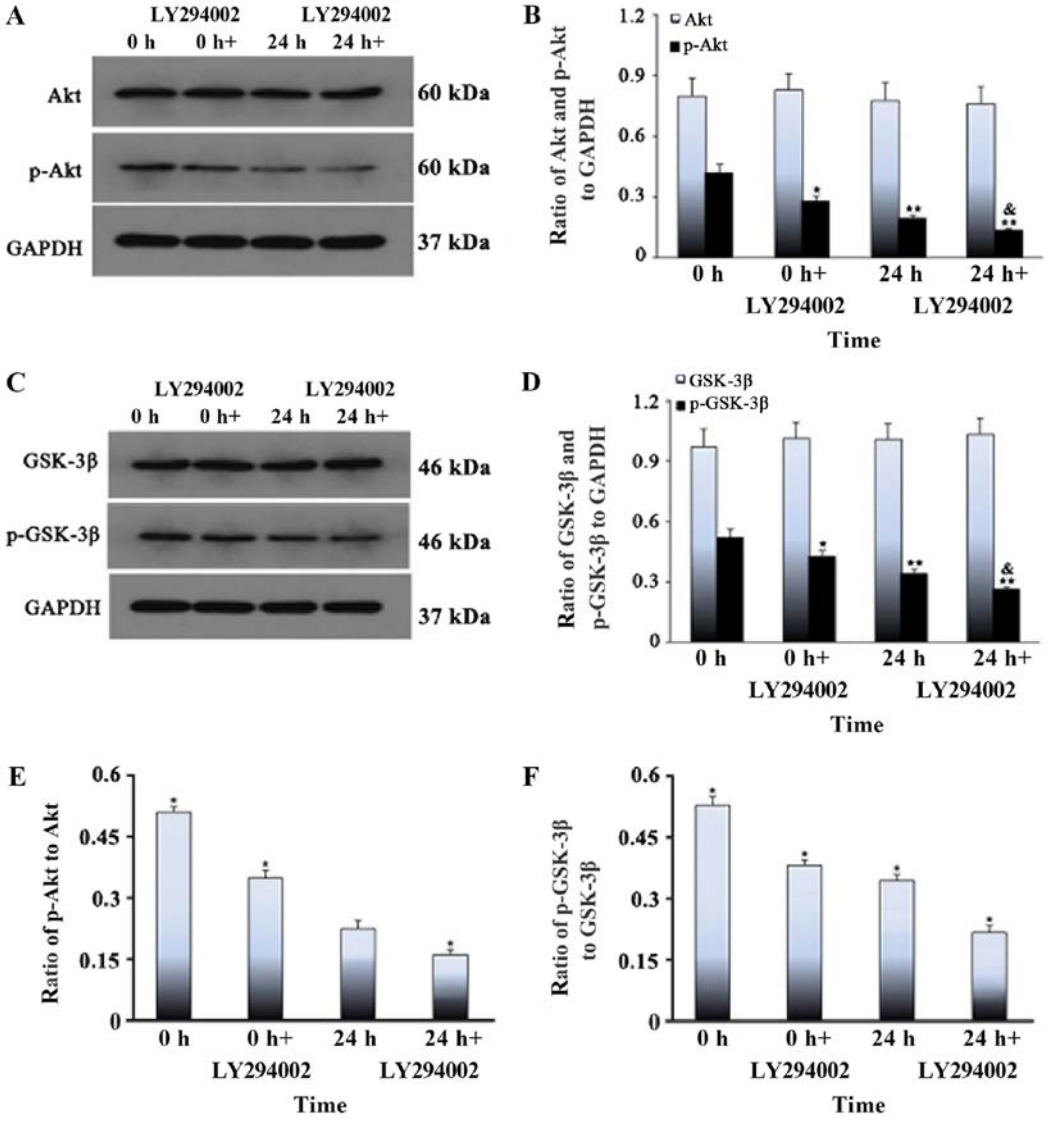

Figure 8. Effect of PI3K/Akt signaling inhibitor LY294002 on the levels of Akt, p-Akt, GSK-3β and p-GSK-3β in rat L6 myoblasts. Protein expression was examined after continuous stretch for 24 h; 20 μM of LY294002 (2 μl/well) was added to the cells 2 h before initiation of stretching. Cells were harvested at 24 h and western blotting was performed. (A) Western blotting results of (B) p-Akt expression; levels were lower in cells treated with LY294002 than in cells stretched for 24 h, but total Akt protein level did not differ among groups. (C) Western blotting results of (D) GSK-3β expression, which did not differ between LY294002-treated cells and cells stretched for 24 h in the absence of inhibitor, but p-GSK-3β level exhibited a trend similar to p-Akt following inhibitor treatment. Ratio of (E) p-Akt to Akt and (F) the ratio of p-GSK-3β to GSK-3β. Values represent mean ± SD of three experiments. *P<0.05 vs. control; **P<0.01 vs. control; $^{\&}$P<0.05 vs. 24 h. p-, phosphorylated; GSK-3β, glycogen synthase kinase 3β.

roles in oxidative stress-induced neuronal apoptosis (37), is negatively regulated by Akt activity.

PI3K is involved in the regulation of various intracellular functions, such as glucose transport, cell proliferation, differentiation and apoptosis (22). After PI3K is activated, three products are produced. One of the products, phosphatidylinositol (2,4,5)-triphosphate, acts as a second messenger, binding to Akt to activate it and translocate it to the cell membrane (38). Akt is a serine/threonine protein kinase, also known as protein kinase B. Activated Akt activates or inhibits downstream target proteins through phosphorylation, thereby regulating cell proliferation, differentiation and survival (22). Therefore, the signaling pathway composed of PI3K and Akt plays a key role in regulating cell proliferation and survival (38). GSK-3β is also a serine/threonine protein kinase and is involved glucose metabolism regulation, as well as numerous other functions (39). A growing body of research has found that GSK-3β phosphorylates a variety of substrates and is involved in a variety of cellular processes, including regulation of the cell cycle and apoptosis, regulation of gene transcription and protein expression, and the maintenance of cytoskeletal integrity (40). It has been shown that activation of GSK-3β further activates apoptosis-associated protein kinases (41). The activity of GSK-3β is mainly dependent on its phosphorylation status. Unlike most other kinases, p-GSK-3β is the inactive state of GSK-3β (42). The phosphorylation status of GSK-3β is mainly regulated by Akt, and various stimulating factors activate the PI3K/Akt pathway, phosphorylating GSK-3β to inactivate it and thereby inhibit apoptosis (43). In models of cardiac, cerebral and renal ischemia, ischemic treatment enhanced the phosphorylation of Akt and GSK-3β

(Ser9) by activating the PI3K/Akt/GSK-3β signaling pathway and exerting its antiapoptotic effect (44,45). Previous studies have also found that activated GSK-3β can induce the opening of the MPTP, thereby promoting cell apoptosis. By inhibiting the activity of GSK-3β, the opening of the MPTP can be prevented, thereby inhibiting apoptosis (46,47).

In the present study, a cell model of mechanical stretch-induced myoblast apoptosis was established and used to elucidate how PI3K/Akt signaling modulates this process. Specifically, cells were treated with the pathway-specific inhibitor, LY294002, to block PI3K/Akt signaling. Hoechst 33258 staining revealed that LY294002 increased apoptosis compared with the 24 h stretch without inhibitor group, while the proportion of apoptotic cells was highest in the 24 h stretch + inhibitor group. These observations indicated that LY294002 promoted cyclic stretch-induced apoptosis, in accordance with the results of flow cytometry assays. WB revealed that levels of the phosphorylated proteins, p-Akt and p-GSK-3β were reduced in PI3K/Akt signaling, indicating that PI3K/Akt signaling is involved in stretch-induced apoptosis. No difference was observed between the total levels of Akt and GSK-3β proteins after the addition of PI3K inhibitors. Together, these findings suggested that myoblast apoptosis induced by cyclic stretch is related to the phosphorylation levels of Akt and GSK-3β, and that the phosphorylation level of both proteins is negatively associated with myoblast apoptosis.

In addition, the opening state of the MPTP was investigated. Mitochondrial damage induced by the opening of the MPTP leads to the disruption of cellular functions and eventually causes cell death by inducing the release of apoptogenic factors, depolarizing the transmembrane potential and impairing oxidative phosphorylation (48,49). Moreover, substances that promote MPTP opening can induce apoptosis, whereas substances that prevent its opening can prevent apoptosis (27). In general, changes in mitochondrial membrane potential are used to indirectly detect mitochondrial membrane permeability. However, the increase in mitochondrial membrane permeability occurs before the change in membrane potential. Therefore, direct detection of mitochondrial membrane permeability enables the detection of apoptosis at an earlier stage (50,51). In this experiment, flow cytometry was used to detect the opening of the MPTP. As stretch loading time increased, this may have led to an increase in the intracellular concentration of LY294002, thereby stimulating a gradual increase in mitochondrial membrane permeability and maintaining the MPTP in an open state via the inhibition of PI3K/Akt signaling, consequently leading to an increase in the proportion of apoptotic cells over time. In support of this, it was shown that the fluorescence quenching rate was higher in the inhibitor-treated group than in cells that were simply stretched for 24 h, and was highest in the 24 h stretch + LY294002 treatment group. Furthermore, activation of the mitochondrial apoptosis pathway has been previously associated with the MPTP (52). Collectively, these findings suggested that LY294002 increased myoblast apoptosis by promoting MPTP opening via the PI3K/Akt pathway.

In summary, it was shown in the present study that mitochondria, as the main site of endogenous apoptosis, play important roles in this process. The opening of the MPTP is a key enabling event in mitochondria-mediated apoptosis, and the subsequent decrease of membrane potential is an important feature of early apoptosis. The PI3K/Akt signaling pathway is important for cell proliferation and survival. In cell models under multiple stimulation, the PI3K/Akt signaling pathway has been shown to be an important factor in inhibiting apoptosis and promoting cell survival (53). However, to the best of our knowledge, the role of PI3K/Akt signaling in cyclic stress-induced apoptosis has not been previouly reported. Further investigation of this will help clarify the mechanisms underlying adaptive reconstruction of facial and maxillary muscles during functional correction, and thereby provide a theoretical basis for clinical observations.

The limitations of the present study are as follows: i) Although Akt, a target for PI3K kinase activation, is a key signaling molecule for the PI3K/Akt/GSK-3β signaling pathway, thus investigations are required to detect PI3K in subsequent experiments; and ii) only one PI3K inhibitor was used to treat the cells when observing the morphological changes and apoptosis of myoblasts, and the specificity of this inhibitor may be lower than that of RNAi technology. In future validation studies, it would be beneficial to use RNAi technology to inhibit the PI3K/Akt/GSK-3β pathway.

Acknowledgements

Not applicable.

Funding

The current study was supported by the National Natural Science Foundation of China (grant no. 31870929).

Availability of data and materials

The datasets used and/or analyzed during the current study are available from the corresponding author on reasonable request.

Authors' contributions

XH, XYa, XYu, ML, QiaZ and YT conceived and designed the experiments. YT, FW and XYa performed the experiments. QiaZ, JC, QiZ acquired the data. JC and QiZ analyzed and interpreted the data. ML, QiZ, YT and XH drafted the manuscript. QiaZ, ML and XYu reviewed and edited the manuscript. QiaZ and XYu supervised the study. All authors read and approved the final manuscript.

Ethics approval and consent to participate

Not applicable.

Patient consent for publication

Not applicable.

Competing interests

The authors declare that they have no competing interests.

References

1. Proske U and Morgan DL: Muscle damage from eccentric exercise: Mechanism, mechanical signs, adaptation and clinical applications. J Physiol 537: 333-345, 2001.
2. Thiruvenkatachari B, Harrison J, Worthington H and O'Brien K: Early orthodontic treatment for Class II malocclusion reduces the chance of incisal trauma: Results of a Cochrane systematic review. Am J Orthod Dentofacial Orthop 148: 47-59, 2015.
3. DiBiase AT, Cobourne MT and Lee RT: The use of functional appliances in contemporary orthodontic practice. Br Dent J 218: 123-128, 2015.
4. O'Brien K, Wright J, Conboy F, Sanjie Y, Mandall N, Chadwick S, Connolly I, Cook P, Birnie D, Hammond M, *et al*: Effectiveness of treatment for Class II malocclusion with the Herbst or twin-block appliances: A randomized, controlled trial. Am J Orthod Dentofacial Orthop 124: 128-137, 2003.
5. Yamin-Lacouture C, Woodside DG, Sectakof PA and Sessle BJ: The action of three types of functional appliances on the activity of the masticatory muscles. Am J Orthod Dentofacial Orthop 112: 560-572, 1997.
6. Tallgren A, Christiansen RL, Ash M Jr and Miller RL: Effects of a myofunctional appliance on orofacial muscle activity and structures. Angle Orthod 68: 249-258, 1998.
7. Haga JH, Li YS and Chien S: Molecular basis of the effects of mechanical stretch on vascular smooth muscle cells. J Biomech 40: 947-960, 2007.
8. Seale P and Rudnicki MA: A new look at the origin, function, and 'stem-cell' status of muscle satellite cells. Dev Biol 218: 115-124, 2000.
9. Hawke TJ and Garry DJ: Myogenic satellite cells: Physiology to molecular biology. J Appl Physiol (1985) 91: 534-551, 2001.
10. Tan J, Kuang W, Jin Z, Jin F, Xu L, Yu Q, Kong L, Zeng G, Yuan X and Duan Y: Inhibition of NFkappaB by activated c-Jun NH2 terminal kinase 1 acts as a switch for C2C12 cell death under excessive stretch. Apoptosis 14: 764-770, 2009.
11. Sun K, Liu F, Wang J, Guo Z, Ji Z and Yao M: The effect of mechanical stretch stress on the differentiation and apoptosis of human growth plate chondrocytes. In Vitro Cell Dev Biol Anim 53: 141-148, 2017.
12. Cheng CS, El-Abd Y, Bui K, Hyun YE, Hughes RH, Kraus WE and Truskey GA: Conditions that promote primary human skeletal myoblast culture and muscle differentiation in vitro. Am J Physiol Cell Physiol 306: C385-C395, 2014.
13. Chen R, Liu X, Huang W, Zeng H, Shi D, Cao B and Liao H: Effects of mechanical stimulation on expression of autoantigens in myoblasts. Zhongguo Xiu Fu Chong Jian Wai Ke Za Zhi 27: 1128-1133, 2013 (In Chinese).
14. Liu J, Liu J, Mao J, Yuan X, Lin Z and Li Y: Caspase-3-mediated cyclic stretch-induced myoblast apoptosis via a Fas/FasL-independent signaling pathway during myogenesis. J Cell Biochem 107: 834-844, 2009.
15. Kerr JF: History of the events leading to the formulation of the apoptosis concept. Toxicology 181-182: 471-474, 2002.
16. Fiers W, Beyaert R, Declercq W and Vandenabeele P: More than one way to die: Apoptosis, necrosis and reactive oxygen damage. Oncogene 18: 7719-7730, 1999.
17. Cheng W, Li B, Kajstura J, Li P, Wolin MS, Sonnenblick EH, Hintze TH, Olivetti G and Anversa P: Stretch-induced programmed myocyte cell death. J Clin Invest 96: 2247-2259, 1995.
18. Zhang Y, Zhou H, Wu W, Shi C, Hu S, Yin T, Ma Q, Han T, Zhang Y, Tian F and Chen Y: Liraglutide protects cardiac microvascular endothelial cells against hypoxia/reoxygenation injury through the suppression of the SR-Ca(2+)-XO-ROS axis via activation of the GLP-1R/PI3K/Akt/survivin pathways. Free Radic Biol Med 95: 278-292, 2016.
19. Yang J, Chen L, Yang J, Ding J, Rong H, Dong W and Li X: High mobility group box-1 induces migration of vascular smooth muscle cells via TLR4-dependent PI3K/Akt pathway activation. Mol Biol Rep 39: 3361-3367, 2012.
20. Lee WJ: Insulin-like growth factor-I-induced androgen receptor activation is mediated by the PI3K/Akt pathway in C2C12 skeletal muscle cells. Mol Cells 28: 495-499, 2009.
21. Tang Y, Liu P, Tian Y, Xu Y, Ren F, Cui X and Fan J: Overexpression of ribonuclease inhibitor defines good prognosis and suppresses proliferation and metastasis in human colorectal cancer cells via PI3K/AKT pathway. Clin Transl Oncol 17: 306-313, 2015.
22. Shaw RJ and Cantley LC: Ras, PI(3)K and mTOR signalling controls tumour cell growth. Nature 441: 424-430, 2006.
23. Jie B, Zhang X, Wu X, Xin Y, Liu Y and Guo Y: Neuregulin-1 suppresses cardiomyocyte apoptosis by activating PI3K/Akt and inhibiting mitochondrial permeability transition pore. Mol Cell Biochem 370: 35-43, 2012.
24. Giorgio V, von Stockum S, Antoniel M, Fabbro A, Fogolari F, Forte M, Glick GD, Petronilli V, Zoratti M, Szabó I, *et al*: Dimers of mitochondrial ATP synthase form the permeability transition pore. Proc Natl Acad Sci USA 110: 5887-5892, 2013.
25. Lindsay J, Esposti MD and Gilmore AP: Bcl-2 proteins and mitochondrial-specificity in membrane targeting for death. Biochim Biophys Acta 80: 593-614, 2011.
26. Riedl SJ and Shi Y: Molecular mechanisms of caspase regulation during apoptosis. Nat Rev Mol Cell Biol 5: 897-907, 2004.
27. Claerhout S, Decraene D, Van Laethem A, Van Kelst S, Agostinis P and Garmyn M: Akt delays the early-activated apoptotic pathway in UVB-irradiated keratinocytes via BAD translocation. J Invest Dermatol 127: 429-438, 2007.
28. Jacobs KM, Bhave SR, Ferraro DJ, Jaboin JJ, Hallahan DE and Thotala D: GSK-3β: A bifunctional role in cell death pathways. Int J Cell Biol 2012: 930710, 2012.
29. Wu D and Pan W: GSK3: A multifaceted kinase in Wnt signaling. Trends Biochem Sci 35: 161-168, 2010.
30. Nakayama M, Hisatsune J, Yamasaki E, Isomoto H, Kurazono H, Hatakeyama M, Azuma T, Yamaoka Y, Yahiro K, Moss J and Hirayama T: Helicobacter pylori VacA-induced inhibition of GSK3 through the PI3K/Akt signaling pathway. J Biol Chem 284: 1612-1619, 2009.
31. Liu J, Liu J, Mao J, Yuan X, Lin Z and Li Y: Caspase-3-mediated cyclic stretch-induced myoblast apoptosis via a Fas/FasL-independent signaling pathway during myogenesis. J Cell Biochem 107: 834-844, 2010.
32. Freudlsperger C, Burnett JR, Friedman JA, Kannabiran VR, Chen Z and Van Waes C: EGFR-PI3K-AKT-mTOR signaling in head and neck squamous cell carcinomas: Attractive targets for molecular-oriented therapy. Expert Opin Ther Targets15: 63-74, 2010.
33. Ke F, Wang Z, Song X, Ma Q, Hu Y, Jiang L, Zhang Y, Liu Y, Zhang Y and Gong W: Cryptotanshinone induces cell cycle arrest and apoptosis through the JAK2/STAT3 and PI3K/Akt/NFκB pathways in cholangiocarcinoma cells. Drug Des Devel Ther 11: 1753-1766, 2017.
34. Chang F, Lee JT, Navolanic PM, Steelman LS, Shelton JG, Blalock WL, Franklin RA and McCubrey JA: Involvement of PI3K/Akt pathway in cell cycle progression, apoptosis, and neoplastic transformation: A target for cancer chemotherapy. Leukemia 17: 590-603, 2003.
35. Gu X, Han D, Chen W, Zhang L, Lin Q, Gao J, Fanning S and Han B: SIRT1-mediated FoxOs pathways protect against apoptosis by promoting autophagy in osteoblast-like MC3T3-E1 cells exposed to sodium fluoride. Oncotarget 7: 65218-65230, 2016.
36. Sussman M: 'AKT'ing lessons for stem cells: Regulation of cardiac myocyte and progenitor cell proliferation. Trends Cardiovasc Med 17: 235-240, 2007.
37. Long ZM, Zhao L, Jiang R, Wang KJ, Luo SF, Zheng M, Li XF and He GQ: Valproic acid modifies synaptic structure and accelerates neurite outgrowth via the glycogen synthase kinase-3β signaling pathway in an Alzheimer's disease model. CNS Neurosci Ther 21: 887-897, 2015.
38. Osaki M, Oshimura M and Ito H: PI3K-Akt pathway: Its functions and alterations in human cancer. Apoptosis 9: 667-676, 2004.
39. Ali A, Hoeflich KP and Woodgett JR: Glycogen synthase kinase-3: Properties, functions, and regulation. Chem Rev 101: 2527-2540, 2001.
40. Cohen P and Frame S: The renaissance of GSK3. Nat Rev Mol Cell Biol 2: 769-776, 2001.
41. Zhang X, Jiang W, Zhou AL, Zhao M and Jiang DR: Inhibitory effect of oxymatrine on hepatocyte apoptosis via TLR4/PI3K/Akt/GSK-3β signaling pathway. World J Gastroenterol 23: 3839-3849, 2017.
42. Embi N, Rylatt DB and Cohen P: Glycogen synthase kinase-3 from rabbit skeletal muscle. Separation from cyclic-AMP-dependent protein kinase and phosphorylase kinase. Eur J Biochem 107: 519-527, 1980.

43. Cai Z and Semenza GL: Phosphatidylinositol-3-Kinase signaling is required for erythropoietin-mediated acute protection against myocardial ischemia/reperfusion injury. Circulation 109: 2050-2053, 2004.
44. Linseman DA, Butts BD, Precht TA, Phelps RA, Le SS, Laessig TA, Bouchard RJ, Florez-McClure ML and Heidenreich KA: Glycogen synthase kinase-3beta phosphorylates Bax and promotes its mitochondrial localization during neuronal apoptosis. J Neurosci 24: 9993-10002, 2004.
45. Sharples EJ, Patel N, Brown P, Stewart K, Mota-Philipe H, Sheaff M, Kieswich J, Allen D, Harwood S, Raftery M, *et al*: Erythropoietin protects the kidney against the injury and dysfunction caused by ischemia-reperfusion. J Am Soc Nephrol 15: 2115-2124, 2004.
46. Pap M and Cooper GM: Role of translation initiation factor 2B in control of cell survival by the phosphatidylinositol 3-kinase/Akt/glycogen synthase kinase 3beta signaling pathway. Mol Cell Biol 32: 578-586, 2002.
47. Bopassa JC, Ferra R, Gateau-Rosech O, Couture-Lepetit E and Ovize M: PI 3-kinase regulates the mitochondrial transition pore in controlled reperfusion and postconditioning. Cardiovasc Res 69: 178-185, 2006.
48. Liu XH, Aksan A, Menze MA, Hand SC and Toner M: Trehalose loading through the mitochondrial permeability transition pore enhances desiccation tolerance in rat liver mitochondria. Biochim Biophys Acta 1717: 21-26, 2005.
49. Ly JD, Grubb DR and Lawen A: The mitochondrial membrane potential (deltapsi(m)) in apoptosis; an update. Apoptosis 8: 115-128, 2003.
50. Quan JH, Cha GH, Zhou W, Chu JQ, Nishikawa Y and Lee YH: Involvement of PI 3 kinase/Akt-dependent Bad phosphorylation in Toxoplasma gondii-mediated inhibition of host cell apoptosis. Exp Parasitol 133: 462-471, 2013.
51. Gardai SJ, Hildeman DA, Frankel SK, Whitlock BB, Frasch SC, Borregaard N, Marrack P, Bratton DL and Henson PM: Phosphorylation of Bax Ser184 by Akt regulates its activity and apoptosis in neutrophils. J Biol Chem 279: 21085-21095, 2004.
52. Fu M, Wan F, Li Z and Zhang F: 4SC-202 activates ASK1-dependent mitochondrial apoptosis pathway to inhibit hepatocellular carcinoma cells. Biochem Biophys Res Commun 471: 267-273, 2016.
53. Zhou BH, Tan PP, Jia LS, Zhao WP, Wang JC and Wang HW: PI3K/AKT signaling pathway involvement in fluoride-induced apoptosis in C2C12 cells. Chemosphere 199: 297-302, 2018.